

Anticancer and Immunostimulatory Activity by Conjugate of Paclitaxel and Non-toxic Derivative of LPS for Combined Chemo-immunotherapy

Aniruddha Roy · Sourav Chandra · Swapna Mamilapally · Pramod Upadhyay · Sangeeta Bhaskar

Received: 26 December 2011 / Accepted: 11 April 2012 / Published online: 1 May 2012
© Springer Science+Business Media, LLC 2012

ABSTRACT

Purpose Cancer is a multifactorial syndrome; hence, multidimensional therapy with a chemo-immunotherapeutic conjugate could be more effective in curing the disease.

Methods We used SP-LPS, a bio-polymer having potent immunostimulatory activity, for conjugation with paclitaxel to make a chemo-immunotherapeutic conjugate. Its physicochemical characterization was done by HPLC, NMR and IR spectra. Stability was measured at different pH, temperature and in tissue homogenates. Chemotherapeutic and immunostimulatory activity was evaluated *in vitro* and also in tumor microenvironment.

Results The conjugate self assembled into nanoparticulate structure, probably due to micelle formation. Stability was pH and temperature dependent. The conjugate exhibited chemotherapeutic and immunotherapeutic activity *in vitro*. *In vivo* antitumor activity was significantly higher and a higher percentage of activated immune cells were found in the tumor microenvironment of the conjugate-treated mice as compared to Taxol®-treated group.

Conclusions This conjugate is a potential chemo-immunotherapeutic compound for the treatment of cancer with advantages over present day chemotherapy with Taxol in terms of higher anticancer activity, less toxicity and ease of delivery.

KEY WORDS chemo-immunotherapy · immunostimulation · paclitaxel · polymer-drug conjugate · SP-LPS

INTRODUCTION

Cancer is a major cause of death in the developed and developing countries alike. Chemotherapy, which is generally regarded as the first line approach for the treatment of cancer, becomes ineffective in many patients (1). This might be due to the genetic plasticity of the tumor cells which help a subgroup of cancer cells to mutate and evade the chemotherapy. Increasing dose of the drugs does not guarantee elimination of this subset of tumor cells, but would eventually lead to systemic toxicity. These cells, getting selected in this process, gain resistance against the chemotherapy. To evade the emergence of resistance, it is rational to design a treatment modality where multi-dimensional therapy is possible. Current knowledge suggests that combined chemo-immunotherapeutic regimens can have great potential for improving the clinical outcome of cancer patients (2). In this study we prepared a chemo-immunotherapeutic compound by conjugating a chemotherapeutic drug with an immune stimulant and evaluated its anticancer activity.

Paclitaxel (PTX) is a very promising antineoplastic agent proven to be effective against a wide array of tumors. The drug assist polymerization of tubulin dimmers to a hyperstable and dysfunctional state, thus arresting the cell cycle at the G2/M phase, leading to cell death (3). The use of PTX is however limited due to its poor aqueous solubility. In current commercial formulation of PTX, i.e., Taxol®, PTX is dissolved in 1:1 (v/v) mixture of Cremophor EL and dehydrated alcohol. Several toxic effects have been attributed to Cremophor EL, including serious hypersensitive reactions (4). Lots of

Electronic supplementary material The online version of this article (doi:10.1007/s11095-012-0756-y) contains supplementary material, which is available to authorized users.

A. Roy · S. Chandra · S. Mamilapally · P. Upadhyay (✉) · S. Bhaskar (✉)
Product Development Cell-I, National Institute of Immunology
Aruna Asaf Ali Marg, New Delhi 110067, India
e-mail: pkumar@nii.res.in
e-mail: sangeeta@nii.res.in

Present Address:
S. Mamilapally
Celavie Biosciences, LLC
Oxnard, California 93030, USA

attempts have been made for the development of new delivery systems of paclitaxel including parenteral emulsions (5), liposomes (6), micelles (7), polymeric micro/nanoparticles (8), and water-soluble prodrugs (9) with variable success.

Conjugation of PTX to water-soluble macromolecular carriers, such as PEG (Poly-ethylene glycol) (10), PG (poly L-glutamic acid) (11) and human plasma albumin (12) have been studied to make a Cremophor free PTX delivery system. However, as none of these polymers are bioactive, they do not potentiate the antitumor activity of the drug. Conjugating PTX with an immune active polymer not only has the advantages of a polymer – drug conjugate, but might also have combined chemo-immunotherapeutic activity against the tumor. It is well established that growing tumor suppresses the anticancer immune response at its local microenvironment to facilitate its growth (13). Immunotherapy stimulates the immune system and thus helps to induce an effective anti-tumor response. When chemotherapy and immunotherapy are used together, they potentiate each other to exert a synergistic effect (14). Tumor cell death induced by chemotherapy enhances cross-priming of immune cells by providing them with important cancer specific antigens (15), thereby increasing the antitumor T cell response. Immune tolerance and regulation induced by tumor cells can be manipulated by chemotherapy (16) to generate a more potent immune activation with immunotherapy when combined chemo-immunotherapeutic approach is used. Hence a conjugate of PTX with an immune active water soluble polymer could have advantage over present PTX formulation in terms of Cremophor free delivery as well as synergistic chemotherapeutic and immunotherapeutic activity which might results in better prognosis of the disease.

Bacterial lipopolysaccharide (LPS) is a potent immunostimulatory polymeric molecule which activates macrophages which in turn activate T cells for an antitumor immune response (17). Activated macrophages can also be directly cytotoxic to cancer cells by production of TNF- α and Nitric Oxide (18). Macrophages constitute one of the major population of immune cells inside the tumor, attracted to the tumor microenvironment by cytokines and chemokines such as CSF-1 and CCL2 (19). Macrophages exhibit polarity in terms of activation. Classically activated macrophages (M1) and alternatively activated macrophages (M2) represent two extremes in the spectrum of the macrophage phenotype (20). M2 macrophages are immunosuppressive in nature and produce high amounts of IL-10, express scavenger receptors, and exhibit anti inflammatory and tissue repair functions (21). In contrast, M1 macrophages, produced due to activation by microbial products like LPS, secrete large amounts of proinflammatory

cytokines, express high levels of MHC molecules and are potent killers of pathogens and tumor cells (20). Tumor-associated macrophages (TAMs) closely resemble M2 type macrophages (22) and due to their immunosuppressive nature, they promote the cancer cell survival, proliferation, and dissemination. Stimulating these otherwise suppressed, M2 type macrophage to M1 type can be an effective and novel therapeutic approach for cancer treatment that complements chemotherapy.

LPS is a potent stimulator of macrophages but due to its systemic toxicity, it is of limited use in clinical setup. Several detoxified LPS derivatives have been prepared like OM-174, ONO-4007, Monophosphoryl Lipid A (MPL), and 7-Acyl Lipid A (23). One of such derivative is SP-LPS, (24) which is a high molecular weight, sodium phthalate salt of parent LPS, which has been used in this study. It was demonstrated that esterification of LPS with acid anhydrides reduce the toxicity (25) of the parent LPS. Based on this principle, Schenck *et al.* (26) reported the synthesis of SP-LPS by esterification of LPS with phthalic anhydride. McIntire *et al.* (24) reported that this LPS derivative is 10,000 times less toxic than the parent LPS. SP-LPS has been used in many clinical studies and in a human clinical trial of HCG vaccine, it has shown good adjuvant effect (27).

Previously we have reported a nanoparticle dosage form co-encapsulating both PTX and SP-LPS which exhibited encouraging *in vitro* results for combined chemo-immunotherapy (14). But because of suboptimal encapsulation of SP-LPS in the nanoparticles, *in vivo* anti tumor activity of the nanoparticle formulation was not significantly different from PTX alone (unpublished data). In the present study, we report the synthesis of a conjugate of PTX and SP-LPS (PLC). The rationale for designing the conjugate was to develop a single chemical entity of polymeric nature which will not only have the advantage of a polymer-drug conjugate, but would also demonstrate synergistic chemotherapeutic and immunotherapeutic activity against cancer. The conjugate was characterized by NMR and IR spectra. The conjugate was shown to self-assemble to form spherical nanoparticles in aqueous solution as characterized by Dynamic Light Scattering (DLS) and Transmission Electron Microscopy (TEM). Pharmacological activity of the conjugate was studied in *in vitro* model to establish the bioactivity of both PTX and SP-LPS in terms of direct cytotoxicity and immune stimulation respectively. The *in vivo* antitumor activity of the conjugate was compared with commercial formulation of PTX (Taxol®) and SP-LPS solution. The tumor infiltrating mononuclear cells were also analyzed for evaluation of immune status at the tumor microenvironment.

MATERIALS AND METHODS

Cell Lines

B16-F10 and J774.1, which are murine melanoma and macrophage cell line respectively, were purchased from ATCC. They were grown in DMEM supplemented with 10 % FBS and 1 % antibiotic antimycotic solution in a 37°C incubator with 5 % CO₂/95 % humidified air. Splenocytes were isolated from C57BL/6 mice.

Animals

Inbred C57BL/6 mice at 6 weeks of age were obtained from the animal facility of the National Institute of Immunology, New Delhi, India. All animal treatments were performed in accordance with the Institutional Animal Ethics Committee's guidelines (Project Approval No. IAEC#132/08).

General Materials

Succinic anhydride, phthalic anhydride, 4-dimethylaminopyridine (DMAP), N,N'-dicyclohexylcarbodiimide (DCC), propidium iodide (PI) and lipopolysaccharide (LPS) from *Salmonella enterica* serotype *minnesota* were purchased from Sigma-Aldrich. Intaxel (Taxol®) and pure dry powder of paclitaxel were purchased from Dabur, India and 21CEC Pharma Limited, Shanghai respectively. Dulbecco's modified Eagle's medium (DMEM) and Fetal Bovine Serum (FBS) were obtained from Biological Industries, Israel while 100X Antibiotic Antimycotic solutions and enzyme free cell dissociation buffer were from Himedia. Mouse TNF- α and IFN- γ ELISA kits were from e-Biosciences whereas IL-12, IL-10, IL-1 β ELISA kits were purchased from BD Biosciences. Acetonitrile, dichloromethane and ethyl acetate (HPLC grade) were obtained from Merck. Water was purified by reverse osmosis (Milli-Q, Millipore). All the fluorochrome conjugated antibodies for FACS analysis and confocal microscopy were purchased from e-Bioscience.

Conjugation of Paclitaxel with a Non Toxic Derivative of LPS

Preparation of Paclitaxel Succinate

Succinate derivative of PTX was prepared according to Dosio *et al.* (12). Briefly, 20 mg PTX, 200 mg succinic anhydride and 2 mg DMAP was reacted in 2 mL anhydrous pyridine for 5 h at room temperature (Step I, Fig. 1). Pyridine was removed in rota-vac and the dry PTX succinate was further purified by crystallization using acetone-water.

Conjugation of Paclitaxel Succinate with LPS

The free -COOH group of PTX succinate (Step II, Fig. 1) was conjugated with free -OH group of the sugar units of LPS by Steglich esterification method (28). Briefly, 20 mg of PTX succinate was reacted with 20 mg LPS, 5 mg DCC and 2 mg DMAP in 2 mL DMSO (Step II, Fig. 1). The reaction mixture was then dialyzed using a 3.5 kDa dialysis membrane to remove any unreacted compounds. The dialyzed solution was then lyophilized to get dry powder of PTX succinate - LPS conjugate.

Neutralization of Remaining Free -OH Groups of LPS

20 mg PTX succinate - LPS conjugate, 200 mg phthalic anhydride and 5 mg DMAP were reacted in 1 mL pyridine and 1 mL formamide (Step III, Fig. 1). The reaction mixture was dialyzed using a 30 kDa cutoff membrane against MQ water to remove any unreacted compounds and lyophilized to get the dry conjugate.

Preparation of SP-LPS

SP-LPS was prepared by the method of McIntire *et al.* (18). Briefly, 10 mg of LPS was reacted with 100 mg of phthalic anhydride for 36 h in 2 mL of a 1:1 mixture of pyridine and formamide. After the completion of the reaction, it was dialyzed using a 30 kDa cutoff membrane, first against Milli Q water, then against 0.1 M sodium bicarbonate and finally against Milli Q water. The dialyzed sample was then lyophilized to obtain dry powdered SP-LPS.

Physico-Chemical Characterization

HPLC Analysis of PTX, PTX-succinate and PLC

The dry powder of PLC, PTX and PTX succinate were dissolved in DMSO. They were analyzed using a Shimadzu UFLP HPLC system. The mobile phase consisted of 60 : 40 (v/v) acetonitrile : water and delivered at a flow rate of 1.0 mL/min. Detection was done at 228 nm. The reverse phase column used was Phenomenex RPC18 column (300 × 5 mm, pore size 5 μ m).

¹H NMR Spectroscopy

PTX, PTX succinate, LPS and PLC were dissolved in DMSO-*d*₆. The NMR spectra of the solutions were then acquired on a Varian Inova 500 to characterize the compounds. The NMR spectra were analyzed using MestRe-C version 2.3a.

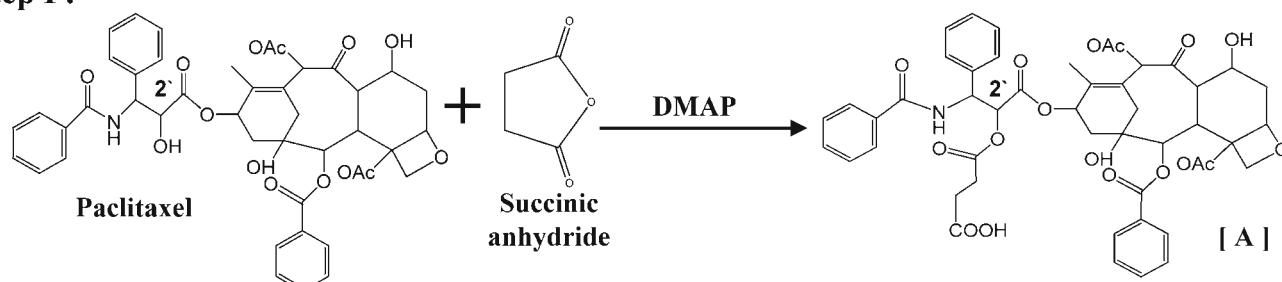
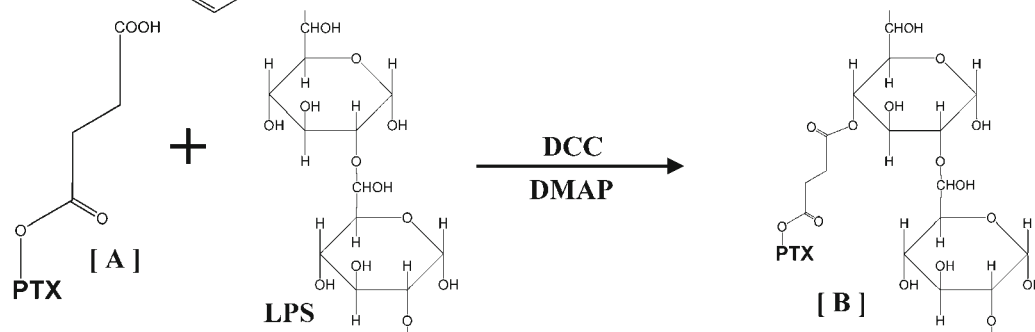
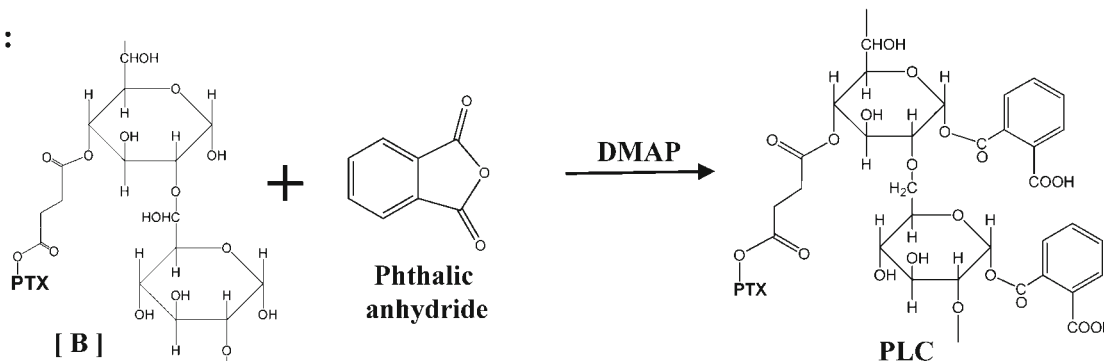
Step I :**Step II :****Step III :**

Fig. 1 Reaction scheme for the preparation of PTX succinate – LPS phthalate conjugate (PLC). In the first step, succinate ester of PTX was prepared using DMAP as the catalyst. In the second step, the free –COOH group of the PTX succinate was conjugated with –OH group of the monosaccharide moieties of LPS. In the last step, remaining free –OH groups of LPS were esterified using phthalic anhydride to make it non toxic. The 2' –OH group of PTX is indicated in the figure.

Fourier Transformed Infrared Spectroscopy

The FTIR spectra for pure PTX succinate, LPS and PLC were obtained from Varian 7000 FTIR for characterizing the chemical nature of PLC. The samples were pressed into a potassium bromide pellet before obtaining their IR absorption spectra. The spectra were detected over a range of 4400–400 cm^{-1} .

Quantification of Paclitaxel in the Conjugate

To quantify the amount of PTX in the conjugate, PLC was dissolved in 100 mM citrate buffer pH 3 and constantly stirred at 72°C for 72 h. Released PTX was extracted with DCM and the DCM extract was dried under vacuum. Residue was redissolved in acetonitrile and concentration of PTX was analyzed using HPLC. The amount of PTX released in this process was considered as total amount of PTX in the conjugate and in all further studies, concentration of PTX in the

conjugate was measured from this. To determine whether total PTX was released from PLC by this method, mass balance analysis was done. PLC was prepared starting with a measured amount of LPS and PTX. The weight of the prepared PLC was measured and it was then dissolved in the hydrolyzing medium (100 mM citrate buffer; pH 3) and after incubating at 72°C for 72 h, it was dialyzed against a 3.5 kDa membrane to remove all the reactants and the released PTX from the backbone LPS. After that, it was lyophilized and the weight of the dry powder was measured. Percentage of PTX released was calculated from the difference between the starting amount of LPS and the amount remaining after the hydrolysis.

Stability Study

The stability of the conjugate was evaluated with respect to temperature, pH and in different physiological

conditions like serum and in different tissue homogenates. 2 mg of conjugate was dissolved in either 50 mM phosphate buffer of pH 7.4 and exposed to different temperature or it was dissolved in 100 mM citrate buffer, pH 3/100 mM carbonate buffer, pH 10/50 mM phosphate buffer, pH 7.4 and kept at room temperature or dissolved in fetal calf serum/tumor homogenate (generated in C57BL/6 mice by s.c. implantation of B16-F10 cell line)/liver homogenate (liver of C57BL/6 mice) and incubated at 37°C. At different time intervals, samples were withdrawn and released PTX was extracted using DCM as described earlier and assayed by HPLC method as described earlier.

Characterization of Self-Assembled Nanoparticles

Size distribution and zeta potential of the self-assembled nanoparticles of PLC were measured at 25°C using a Zetasizer Nano-ZS (Malvern Instruments, UK) after dissolving the conjugate in aqueous solution at a concentration of 5 mg/mL. The morphology of nanoparticles was observed on a Transmission Electron Microscope (TEM), (CM10, Phillips, Holland) after coating the particles with 1 % uranyl acetate over a copper grid (Polysciences, Warrington, PA). TEM images were obtained using software image capture engine (version 5.42.391).

Toxicity Study: Body Weight and Tissue Histology

Toxicity of PLC and PTX were evaluated by the survival on the 7th day after single intravenous injection of different doses in C57BL/6 mice. PLC was dissolved in PBS, whereas PTX was delivered as the commercial formulation diluted in saline. Three different doses of PTX (20 mg/kg; 32 mg/kg and 40 mg/kg) or PLC containing equivalent amount of PTX (50 mg PLC/kg; 80 mg PLC/kg and 100 mg PLC/kg) was used for the toxicity study. Regular checkup of body weight was done for 14 days. Some animals were sacrificed after 48 h of injection and histopathological study was done on different organs to check any indication of toxicity.

Evaluation of Pharmacological Activity in *In Vitro* System

Direct Cytotoxic Activity

0.2 million B16-F10 cells were treated with PTX/PLC containing different concentration of PTX (0.5 and 0.05 µg/mL) for 48 h. Equivalent amount of SP-LPS was used as a control. Cell death was analyzed by PI uptake using flow cytometer (BD LSR, BD Bioscience) and data were analyzed using WinMDI 2.8.

Cell Cycle Arrest Study

For *in vitro* cell cycle arrest study, 0.2 million B16-F10 cells were treated with PTX/PLC at the concentration of 0.25 and 0.025 µg PTX/mL. SP-LPS solution (0.25 µg/mL) was used as a control. After 24 h, cell cycle analysis was done in a flow cytometer (BD LSR, BD Bioscience) after cell permeabilization and PI staining. Data was analyzed using WinMDI 2.8.

Tubulin Binding Study

0.2 million B16-F10 cells were treated with PTX/PLC containing PTX concentration of 0.5 µg/mL. After 24 h of treatment, the cells were fixed and stained with anti-alpha tubulin antibody conjugated with Alexa Fluor 488. The cells were observed under the confocal microscope after mounting with vector shield mounting reagent with DAPI (4',6-diamidino-2-phenylindole).

Macrophage Stimulatory Activity

0.2 million J744.1 cells were treated with SP-LPS solution/PLC containing SP-LPS at a concentration of 0.05 and 0.5 µg/mL. The supernatant was withdrawn after 1, 3, 6, 9 and 12 h and estimated for TNF-α by ELISA.

Splenocyte Activation

Splenocytes were isolated from C57BL/6 mice and stimulated with SP-LPS solution and PLC at a concentration of 0.1 µg SP-LPS/mL. Culture supernatant was withdrawn twice at 18 and 48 h. As TNF-α and IL-12 are secreted by macrophages they were analyzed from the supernatant withdrawn at 18 h while rest of the cytokines IFN-γ, IL-10 and IL-1β were quantitated from the supernatant withdrawn at 48 h.

Co-culture Study

0.2 million B16-F10 cells were labeled with CFSE (Carboxy-fluorescein succinimidyl ester) (5 µM) and co-cultured with 5 million splenocytes isolated from C57BL/6 mice. These were treated with PTX or PLC at the concentration of 0.25 µg PTX/mL. After 24 h, the death of tumor cells was determined by the PI uptake method using flow cytometer (BD LSR, BD Bioscience) after gating on the CFSE labeled cancer cells and data were analyzed using WinMDI 2.8.

Evaluation of *In Vivo* Antitumor Activity

0.5 million B16-F10 melanoma cells were inoculated into the right flank of 6 to 8 weeks old C57BL/6 mice. After 1 week of tumor implantation, animals with an average tumor diameter of 4 – 6 mm were selected. These mice were divided into four treatment groups, taking 8 animals per group and were

numbered. Taxol (10 mg/kg) or SP-LPS (10 mg/kg) or PLC (10 mg PTX equivalent/kg) or saline was administered by peritumoral injection. The drug treatment was continued from day 7 to day 23 with 3 day interval. Total of 5 injections were given (day 7, 11, 15, 19 and 23). The tumor diameters were measured, using a sliding caliper, two or three times per week. The tumor volume (TV) was calculated according to the formula: $TV = (L \times W^2)/2$, where L and W were the length of the major and minor diameters, respectively. One set of treated animals, with 10 animals per group, were observed for 30 days for survival study.

Study of Tumor Infiltrating Lymphocytes for Evaluation of Immune Status of the Tumor Microenvironment

To understand the potential of the conjugate to modulate the immune status of the tumor microenvironment, activation of tumor infiltrating mononuclear cells (TMC) were analyzed. 0.5 million B16-F10 melanoma cells were inoculated in mice and treatment was given as described earlier. After giving treatment till 23rd day of tumor cell inoculation, on 24th day mice were euthanized and the whole tumor was collected. The tumor was enzymatically digested and lymphocytes isolated using Ficoll-paque (GE Healthcare). Cells were finally suspended in PBS and labeled with antibodies to various cell surface markers using standard staining methods. The following panel of commercially available and directly fluorochrome conjugated anti-mouse mAbs were included in the study. FITC anti-mouse CD14, PE anti-mouse CD4, PE anti-mouse CD8, PE anti-mouse CD40, PE anti-mouse CD80 and FITC anti-mouse CD43. Samples were run on a BD LSR (BD Bioscience) flowcytometer and analysed using WinMDI 2.9 software.

Statistical Analysis

Data are presented as the mean \pm standard deviation except for Figs. 8a, c and 9 where it is expressed as mean \pm standard error of the mean. Statistical analyses were performed by a two-tailed student *t*-test. Survival statistics was analyzed using Kaplan-Meier method. Comparison of the survival curves were done by Log-rank (Mantel–Cox) test and Logrank test for trend. The statistical analysis was performed with GraphPad InStat and GraphPad Prism software (GraphPad Software Inc.).

RESULTS

Preparation and Physicochemical Characterization of the Conjugate

The conjugate was prepared by the reaction schemes as depicted in Fig. 1. First PTX succinate [A] was prepared

by the reaction of excess succinic anhydride with PTX. Prepared PTX succinate was isolated and purified from the unreacted succinic anhydride by crystallization (Scheme I). The PTX succinate was then conjugated with LPS by Steglich esterification method (Scheme II). Here, succinate was used as the linker moiety between PTX and LPS. The free $-\text{COOH}$ group of PTX succinate was conjugated with the free $-\text{OH}$ group of the monosaccharide units of LPS to make [B]. In the last step, LPS was made nontoxic by reacting phthalic anhydride with [B] (Scheme III). The final PTX – SP-LPS conjugate was designated as PLC.

In order to validate the conjugation, the conjugate was analyzed for the presence of free PTX or PTX succinate by HPLC. The HPLC data established the absence of both PTX and PTX succinate in PLC (Supplementary Material Fig. S1). PTX and PTX succinate were eluted from the column at 7.5 and 4.7 min respectively whereas PLC was eluted at 3.2 min (due to higher polarity) and no overlapping peak with PTX and PTX succinate was detected.

The synthesized PTX - LPS conjugate was also corroborated by ^1H NMR spectra as shown in Fig. 2. Overlapping signals were seen between PTX and PLC, signifying the presence of PTX in the conjugate. The NMR signal for the proton of $2' - \text{OH}$ group appears at $\delta = 3.94$ ppm (29) in native PTX. This peak, which was present in pure PTX, disappeared in PTX succinate, signifying formation of PTX – $2'$ succinate, because this proton reacts with succinic anhydride in the esterification reaction. Due to attachment of succinate in the $2' - \text{OH}$ position, the signal from $2'\text{C}$ proton, which appeared at $\delta = 4.77$ ppm in PTX (29), also showed shifting. LPS exhibited mostly overlapping ^1H NMR signals with PTX and PTX succinate. One exclusive peak of LPS at $\delta = 1.2$ ppm was also present in the conjugate, suggesting presence of LPS in PLC.

Conjugation was further validated by the IR spectra (Fig. 3). Aliphatic amines absorb in the region $3450\text{ cm}^{-1} - 3250\text{ cm}^{-1}$. As PTX and LPS (due to the presence of amine sugars like glucosamine) contain amino groups, IR absorbance in both of them around 3380 cm^{-1} was because of the presence of this group which was also present in the conjugate. The carbonyl group of PTX succinate exhibited a strong absorption band due to ester bond $\text{C}=\text{O}$ stretching at 1730 cm^{-1} (30), which was also present in the conjugate but absent in the LPS. Due to C-N symmetrical stretching, PTX succinate, LPS and PLC showed a band at 1255 cm^{-1} , 1237 cm^{-1} and 1244 cm^{-1} respectively. The band at 713 cm^{-1} of PTX succinate lies in the fingerprint band region of PTX (30). No IR absorption was detected in this region by LPS but the conjugate showed an absorption band at 708 cm^{-1} . Interestingly, two new absorption bands, at 1540 cm^{-1} and 1371 cm^{-1} , appeared in the conjugate which were not present in PTX succinate or LPS. Ester bonds are known to show IR absorption in the range $1610 - 1540\text{ cm}^{-1}$ due to asymmetric stretch and $1420 - 1300\text{ cm}^{-1}$ due to symmetric

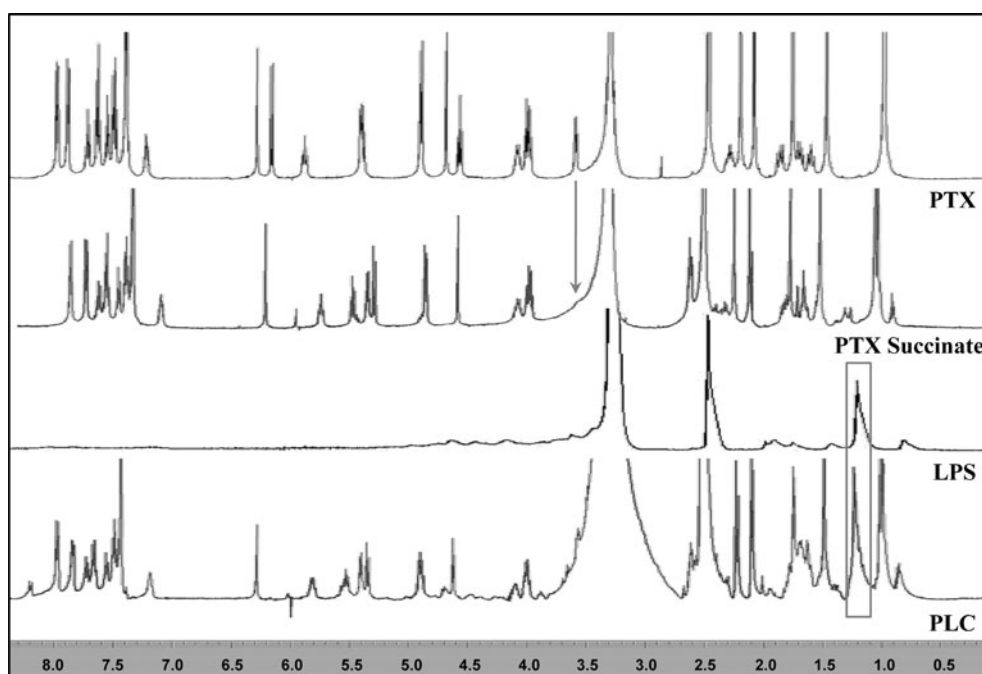


Fig. 2 ^1H NMR spectra of PTX, PTX succinate, LPS and PLC. All of the compounds were dissolved in DMSO- d_6 and the spectra were recorded. Peak corresponds to the proton of 2'-OH group of PTX (3.94 ppm) disappeared in PTX succinate (indicated by an arrow) signifying formation of PTX 2' succinate. The proton peak of 2' C of PTX (4.77 ppm) also shifted in PTX succinate due to formation of ester bond at 2' position. Common peaks between PTX succinate and PLC signified presence of PTX in PLC. LPS exhibited mostly overlapping peaks with PTX succinate. One exclusive peak present in LPS as well as PLC is indicated by a box.

stretch (31). These two new peaks might be due to the formation of the ester linkage between PTX succinate and LPS, confirming formation of the conjugate.

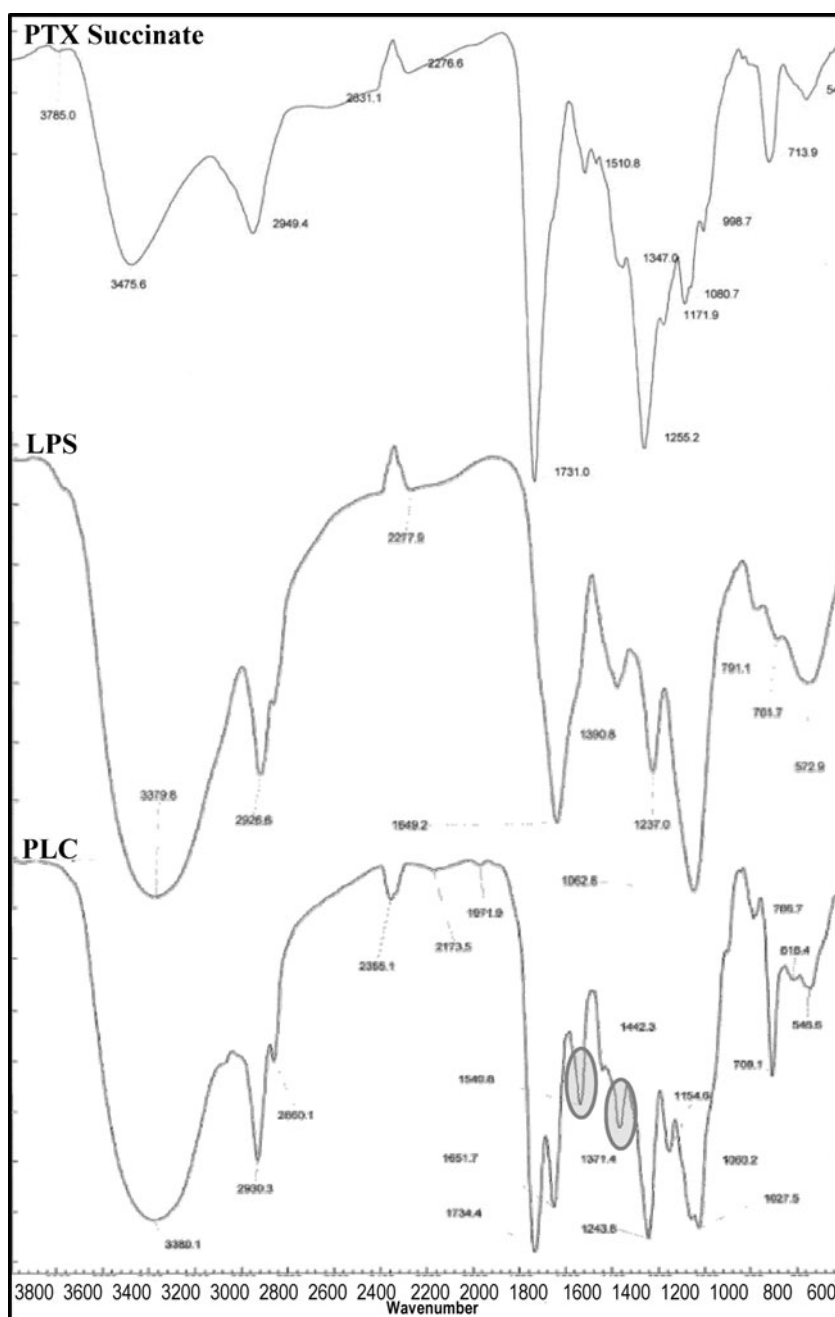
The amount of PTX conjugated in PLC was determined by quantifying the amount of the released drug with acid hydrolysis (pH 3) at higher temperature (72°C) for 72 h. Acid hydrolysis was chosen as PTX is stable at acidic pH than alkaline pH (32). No significant degradation of PTX alone was found when incubated at this pH and temperature for 72 h which is corroborated by other studies (33). Quantification of PTX was done using this indirect method as radioactive PTX was not available. From the mass balance analysis, it was estimated that 97 % of PTX was released from the PLC by this method. We got a conjugation of 0.42 ± 0.03 mg of PTX/mg of PLC. This amount was considered as the total conjugated PTX per mg of PLC and in all further experiments, quantification of total PTX was done based on this. PLC was found to be quite stable at room temperature and at normal physiological pH (Fig. 4a). About 22 % of total PTX got released after incubating at room temperature for 72 h at pH 7.4. Stability was found to be higher when kept at 4°C (Fig. 4b). Stability of PLC was found to be dependent on pH with moderately higher amount of PTX released at pH 3 (≈ 60 %; Fig. 4a) than pH 10 (≈ 56 %; Fig. 4a). Hydrolysis of PLC was found to be higher in tissue homogenates as compared to serum (Fig. 4c).

The conjugate was found to self-assemble into nanoparticulate structures when added in aqueous solution. The average diameter of the particles was measured by Dynamic Light Scattering (DLS) and found to be 215 ± 5 nm (Fig. 5a). The size and shape of the particles was reconfirmed by Transmission Electron Microscopy (TEM) where it was established that the particles are smoothly spherical in nature with a narrow size distribution (Fig. 5c). The particles were negative in charge, with a zeta potential of -31 mV (Fig. 5b).

Toxicity Study

Acute toxicity of the conjugate was analyzed in comparison with PTX. The maximum tolerated dose of PLC was found to be more than 100 mg of PLC/kg (which is equivalent to 40 mg PTX/kg) and that of PTX was 20 mg/kg. When body weight of animals which were given i.v. injection of 20 mg/kg of PTX or PLC containing equivalent amount of PTX were compared, no significant difference in body weight was found (Supplementary Material Fig. S2a). Histopathological study was done after 48 h of treatment with PLC (20 mg PTX equivalent/kg) to check any hypersensitive and inflammatory reaction at the tissue level as LPS exert its toxicity mainly due to hypersensitive reaction which manifests early after administration. The tissue histology of different organs showed no indication of toxicity in the PLC treated mice (Supplementary Material Fig. S2b). As both PTX and PLC were non-toxic at

Fig. 3 Fourier transformed infrared spectra of PTX succinate, LPS and PLC. Overlapping peaks from both PTX succinate and LPS were seen in PLC, suggesting presence of both of them in PLC. Two unique peaks in PLC indicating formation of the ester bond between PTX succinate and LPS are indicated with circles.



the dose of 20 mg PTX equivalent/kg, they did not produce any visible change at the tissue level.

Evaluation of Pharmacological Activity of PLC in *In Vitro* System

Direct Cytotoxic Activity

Pharmacological activity of the conjugate was evaluated in *in vitro* system to confirm the retainment of bioactivity of both

PTX and SP-LPS in the conjugate. Both PTX and PLC exhibited similar dose dependent cytotoxicity (Fig. 6a).

Cell cycle arrest study was done to confirm the mode of action of the conjugate. PTX is known to arrest cell cycle at G2/M phase followed by apoptosis. Similar proportion of G2/M phase arrested population and similar dose dependency was seen in both PTX and PLC treatment (Fig. 6b).

To further investigate whether the cytotoxicity of the conjugate was via the same pathway as that of PTX, tubulin binding study was performed. PTX binds with $\beta 2$ subunit of

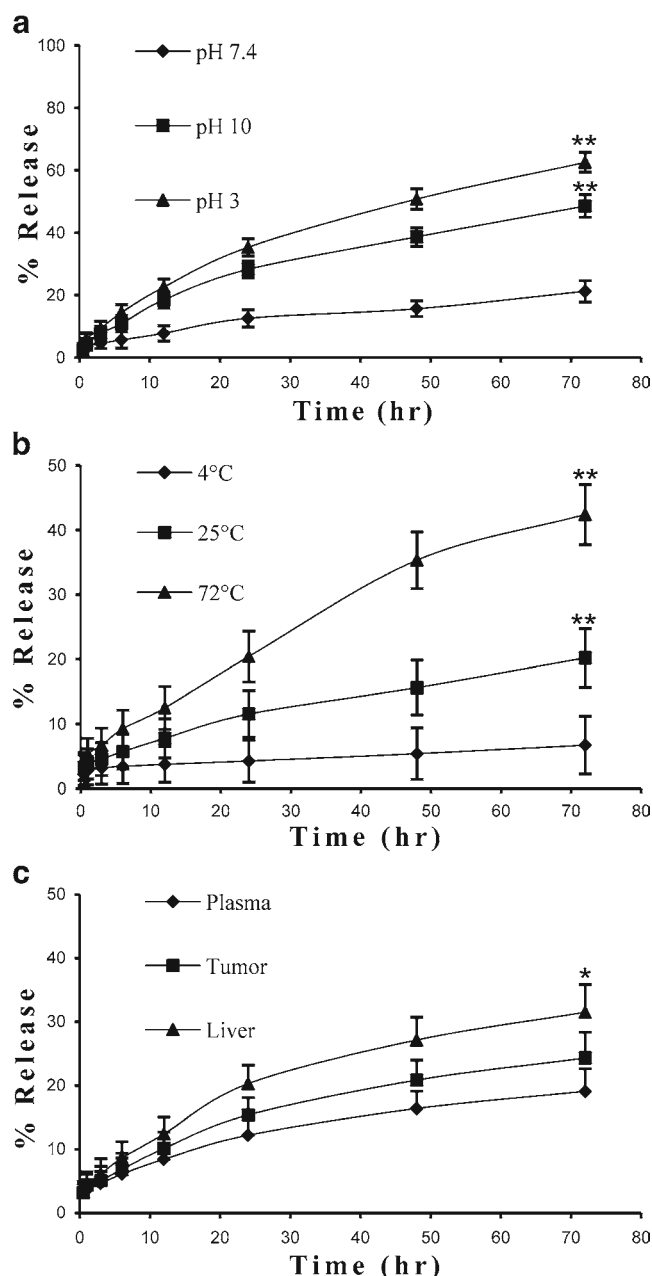


Fig. 4 Stability of PLC at different pH, temperature and in tissue homogenates. Percentage release of PTX from PLC was determined after: **(a)** PLC was dissolved in buffer of different pH and incubated at room temperature, **(b)** PLC was incubated at different temperatures dissolved in phosphate buffer (pH 7.4), **(c)** PLC suspended in plasma or in different tissue homogenates and incubated at 37°C. At specific time points, samples were withdrawn and PTX extracted from it using DCM. The extract was quantified for the amount of PTX by HPLC. PLC was found to be stable at room temperature and release of the drug was dependent on pH and temperature. * $p < 0.05$; ** $p < 0.01$, comparison was done with values at pH 7.4, 4°C and in plasma in respective figures.

tubulin monomer to promote polymerization. When B16-F10 cells were treated with PTX or PLC and then labeled

with anti-tubulin antibody, similar pattern of bunched tubulin was visible around the nuclei in both the treatment groups (Fig. 6c). In contrast, in the control cells normal network of tubulin was seen. Moreover, nuclei of the PTX and PLC treated cells were found to be fragmented in contrast to normal circular nuclei of the control cells. These results established that PLC retained the biological activity of PTX and acts via the same mechanism.

Immunostimulatory Activity

To analyze the immune activity of the conjugate, macrophage stimulatory activity of PLC was studied. Similar amount of TNF- α was detected from J774.1 macrophage cells treated with PLC or SP-LPS, which was significantly higher than that released by PTX treatment (Fig. 7a). To confirm this, activation of splenocytes was also evaluated. Significantly higher amount of Th1 cytokines like TNF- α , IL-12 and IFN- γ were detected in the culture supernatant of splenocytes treated with both PLC and SP-LPS in comparison with PTX and control (Fig. 7b). Another stimulatory cytokine, IL-1 β , was also secreted in a moderate amount in the PLC and SP-LPS treated groups. Secretion of immune regulatory cytokine IL-10 was found to be very low in the treated and control groups. These results established that PLC can effectively modulate the immune cells to an activated state to induce an efficient anti-tumor response.

Co-culture Study to Establish Chemo-immunotherapeutic Activity

After demonstrating the activity of both PTX and SP-LPS in the conjugate, the hypothesis of combined chemo-immunotherapy was confirmed by the coculture analysis, where CFSE labelled B16-F10 cells were co-incubated with splenocytes derived from C57BL/6 mice and given treatment with either PTX, or SP-LPS or PLC. With PLC treatment higher death of the cancer cells was observed as compared to PTX or SP-LPS treatment (Fig. 7c). As PLC had both cytotoxic as well as immunostimulating activity, these two might be cooperating with each other to produce a synergistic effect to produce higher death in the PLC treated cells.

Evaluation of *In Vivo* Antitumor Activity

The *in vivo* antitumor activity of PLC was studied in a mouse tumor model. Tumor volume was found to be consistently low in PLC treated mice as compared to with both Taxol and SP-LPS treated groups (Fig. 8a, b). The higher antitumor activity of PLC over PTX was

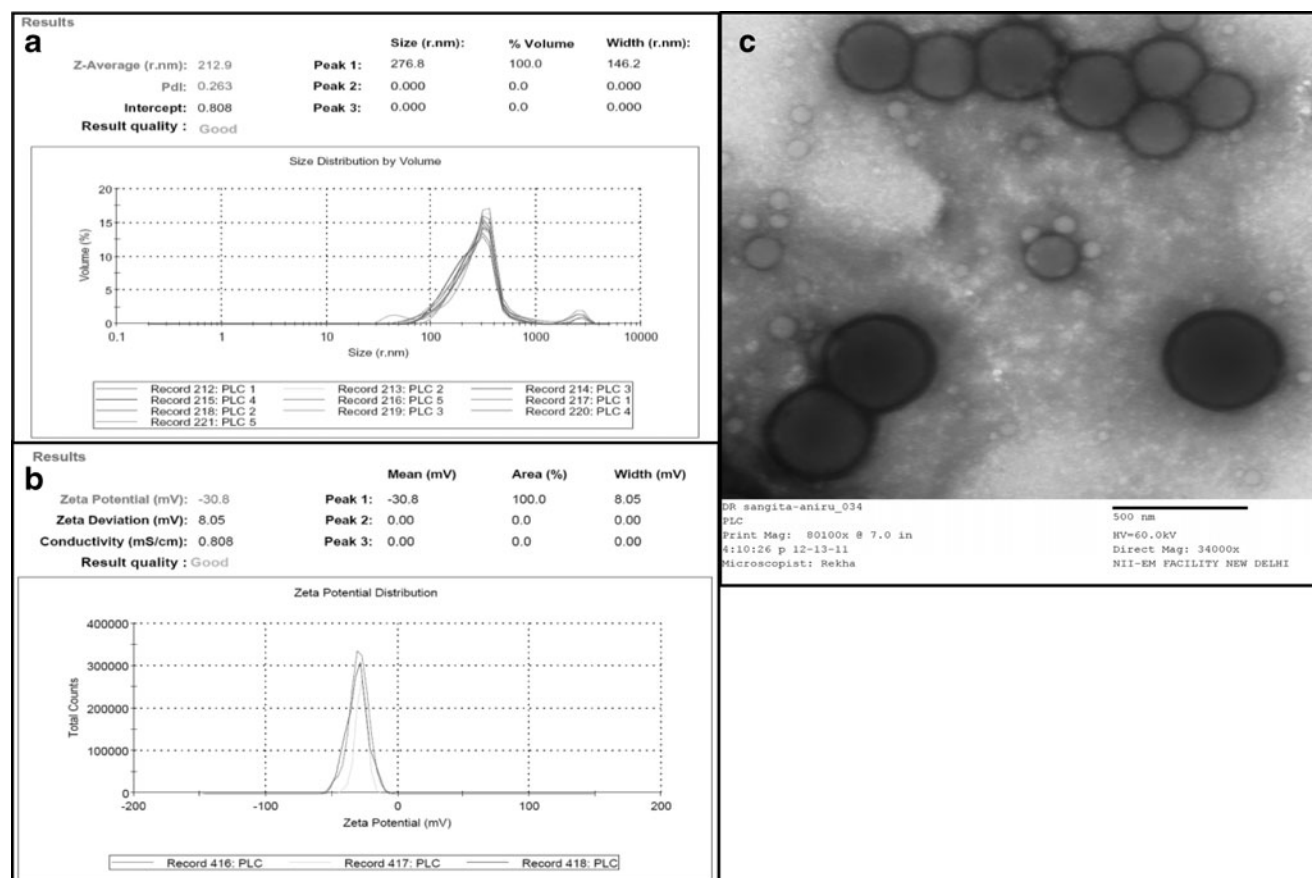


Fig. 5 (a) Size distribution, (b) zeta potential and (c) transmission electron microscopic image of self-assembling nanoparticles of PLC.

also evident from the survival study. About 80 % of tumor bearing mice treated with PLC survived 30 days after treatment whereas only 50 % of PTX treated and 20 % of SP-LPS treated mice survived that long (Fig. 8c). All of the control mice died within 26 days. By Kaplan-Meier analysis, the median survival time of PLC treated animals was found to be more than that of PTX treated animals. These data suggest that combined chemo-immunotherapy with PLC had better anticancer efficacy as compared to commercial Taxol.

Study of Tumor Infiltrating Lymphocytes for Evaluation of Immune Status of the Tumor Microenvironment

Next we analyzed the underlying mechanism for better anti-tumor response by PLC in terms of infiltration and activation of immune cells in the tumor microenvironment. A general Th1 type of immune activation was observed in the PLC treated mice in comparison with both Taxol and SP-LPS. As shown in the Fig. 9, a significant increase was observed in the percentage of macrophage infiltration (CD14+ cells) in the PLC treated group. When activation status of these macrophage cells were checked, it was observed that expression of

CD40 and CD80, both of which are activation markers of macrophage, was also significantly high in the PLC treated mice. These data suggest that higher number of activated immune cells were infiltrated in the tumor of PLC treated mice. The activation status of the T cells was also analyzed as T cells are the main immune effector cells. CD43 was used as a marker for T cell activation. Higher number of activated CD4 and CD8 T cells was found in the PLC treated mice compared to other groups.

DISCUSSION

Chemo-immunotherapy is an emerging treatment strategy where chemotherapy is integrated with immunotherapy for better prognosis of the disease. Although combined chemo-immunotherapy is known to be better than chemotherapy or immunotherapy alone for the treatment of cancer, very few attempts have been made for developing a conjugate having combined chemo-immunotherapeutic activity (34).

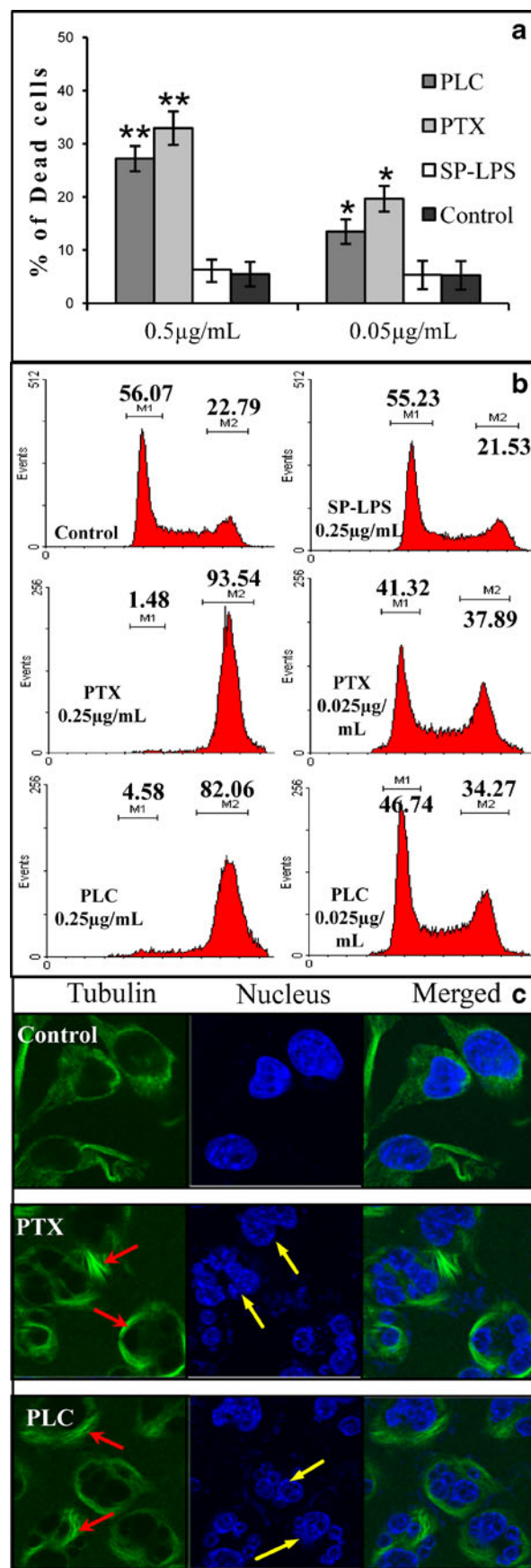
PTX has been shown to enhance the antitumor efficacy of vaccines and helps to induce a tumor specific immune response by the vaccine (35). Zhong *et al.* reported that administration of PTX is associated with beneficial

Fig. 6 Comparison of direct cytotoxicity and cell cycle arresting activity of PLC and PTX. **(a)** Percentage of tumor cell death after treatment with PTX or PLC (containing equivalent amount of PTX) or SP-LPS for 48 hours. **(b)** FACS study of cell cycle arrest after treatment with PLC or PTX or SP-LPS for 24 hours. Values in the M2 region stands for the percentage of G2/M phase arrested population. **(c)** Comparison of tubulin polymerizing activity of PLC and PTX on B16- F10 melanoma cells. Bundled tubulin and fragmented nucleus are indicated with arrows. PLC was found to exert its cytotoxic activity via the same pathway as that of PTX, i.e., formation of hyperstable polymerized tubulin and arresting the cell cycle at the G2/M phase. * $p < 0.05$; ** $p < 0.01$, values compared with control.

alterations of the intratumoral microenvironment and thus support antitumor immunity (36). Based on these studies, we hypothesized that a conjugate of PTX and SP-LPS should exhibit synergistic chemotherapeutic and immunotherapeutic activity. Such a synergism may facilitate a novel treatment modality which could effectively suppress the tumor cell growth. Moreover, as SP-LPS is a hydrophilic polymer, the conjugate was also expected to self assemble in a nanoparticulate structure which could be delivered suspended in PBS, thereby making it a Cremophor free formulation.

The conjugate was synthesized in a 3 step reaction scheme as depicted in Fig. 1. In the first step, PTX was succinylated with succinic anhydride. Succinate group reacted with the 2' –OH group of PTX, as confirmed by the NMR data. It is established from the structure activity relationship study of PTX that the 2' –OH groups of PTX is suitable for modification as esterification in this position does not affect the bioactivity of PTX (37). As a result, most of the PTX derivatives studied by different research groups were modified at this position (10–12). LPS was conjugated with PTX succinate by esterification of the –OH group present in the monosaccharide building blocks of LPS and the free –COOH group of the PTX – succinate. Finally, it was made non toxic by conjugating phthalic anhydride with the remaining free –OH groups of LPS. It is known that toxicity of LPS is reduced when esterified with acid anhydrides (24–26). Phthalate ester of LPS was shown to be 10,000 times less toxic than the parent LPS (24). As it was shown that 20 mg LPS reacts with 0.135 millimole of phthalic anhydride (FW 148) (24), it can be concluded that 20 mg LPS contains 0.135 millimole of esterifiable –OH group. As 20 mg PTX succinate (equivalent to 0.02 millimole, FW 954) was esterified with 20 mg LPS, more than 80 % of the –OH group of LPS should remain free after conjugation with PTX succinate, where further esterification with phthalic anhydride can take place to make the LPS non toxic. Both NMR and IR data confirmed the formation of the final conjugate.

Stability of PLC was found to be temperature and pH dependent. Release of PTX from the conjugate was higher when incubated with liver and tumor homogenate as compared to blood plasma. This observation is similar to other studies where succinate moiety has been used as a linker between PTX and the polymer (12).



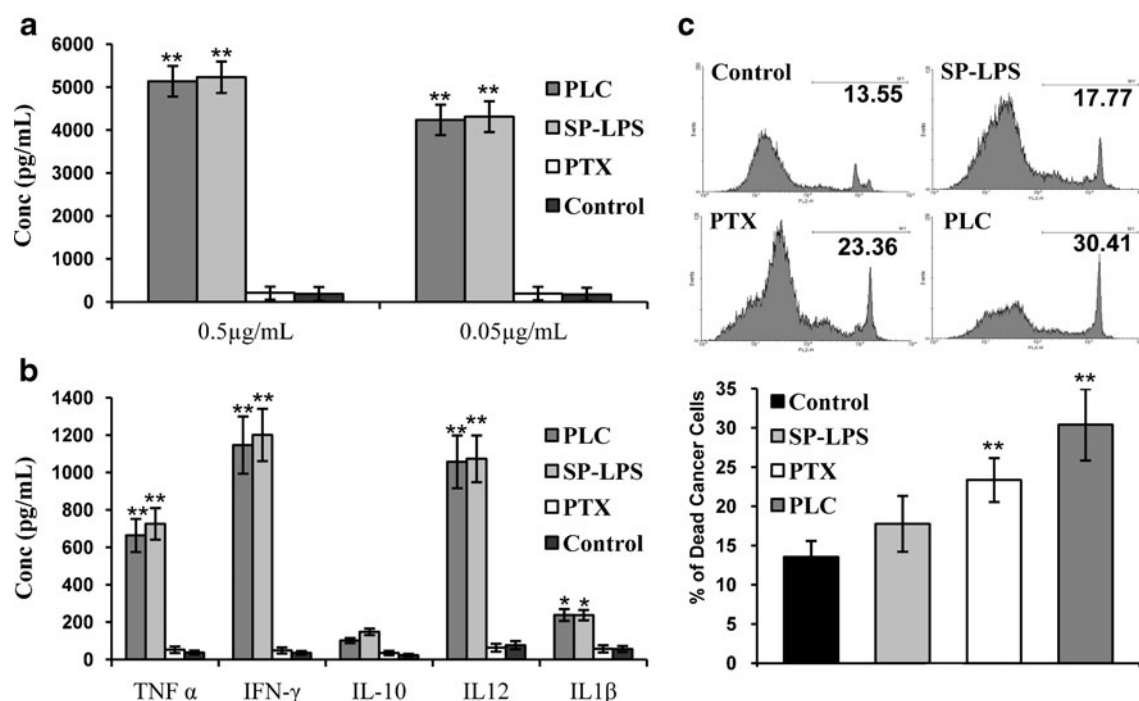


Fig. 7 Comparison of immune stimulatory potency of PLC and SP-LPS and chemo-immunotherapeutic activity of PLC. **(a)** TNF- α secretion by macrophages (J774.1) when stimulated with different doses of SP-LPS or PLC (containing equivalent amount of SP-LPS) or PTX. **(b)** Secretion of different cytokines by splenocytes after stimulation with 0.1 $\mu\text{g/mL}$ of SP-LPS or PLC containing equivalent amount of SP-LPS or 0.1 $\mu\text{g/mL}$ of PTX. Significantly high amount of Th1 cytokines were detected with PLC and SP-LPS treatment. **(c)** Effect of PTX (0.25 $\mu\text{g/mL}$) or PLC containing equivalent amount of PTX on tumor cell death when added in a co-culture of splenocytes and CFSE labeled tumor cells. Target cells were gated and percentage of cell death was analyzed by PI uptake method. Higher death of the target cancer cell with PLC treatment in the immune cell–cancer cell co-culture system suggested the combined chemo-immunotherapeutic activity of PLC * $p < 0.05$; ** $p < 0.01$, values compared with control.

It is reported that amphiphilic conjugates can self-assemble to form nanoparticles in aqueous solution via hydrophobic interactions (38). As PLC is expected to possess amphiphilic characteristics due to the presence of hydrophilic SP-LPS and hydrophobic PTX, we investigated their self-assembling behavior in aqueous solution. The conjugate was indeed found to form nanoparticulate structures in aqueous solution as established by DLS and TEM imaging with an average diameter of 215 ± 5 nm, which is similar to other reported PTX–polysaccharide conjugates (39, 40). As reported by Wang *et al.*, heparin conjugated PTX forms negatively charged (-21 to -31 mV) nanoparticles in aqueous solution (40). Similar to that, the self-assembled particles of PLC had surface charge of -31 mV, probably due to formation of micellar structure where hydrophobic PTX moiety was buried inside while the hydrophilic carboxyl (COO^-) groups of SP-LPS were exposed on the surface, imparting a negative zeta potential. These self-assembling nanoparticles of PLC were likely to have a core/shell structure composed of a hydrophobic inner core containing aggregated PTX molecules and a hydrophilic SP-LPS layer outside the core.

Both PTX and LPS retained their respective bioactivity in the conjugate as confirmed by *in vitro* studies. The conjugate produced its cytotoxic effect via the same pathway as that of PTX, i.e., binding with tubulin and arresting the cell cycle at

the G2/M phase. As the release of PTX from PLC was slow, it seems that the conjugate also contributed to the cytotoxic activity along with the released PTX, which is supported by other reported conjugates of PTX where although the release of PTX from the conjugate is slow, the conjugate showed cytotoxic activity (12, 39). Within 48 hour, about 15 % PTX was released from PLC at room temperature and neutral pH, but similar cytotoxicity was seen with equivalent dose of PTX delivered as PLC or PTX solution, suggesting participation of the intact conjugate in the cytotoxic activity. Polysaccharide coating of nanoparticles facilitate the adhesion of particles to the cell membrane due to their biological adhesion properties (41). In our study, the intra-cellular delivery of PLC might be facilitated due to formation of nanoparticulate micellar structure which had polysaccharide SP-LPS on the surface.

Stimulation of macrophages by PLC treatment established its immunostimulatory activity. We found similar immunostimulatory activity of SP-LPS solution and PLC containing equivalent amount of SP-LPS. As SP-LPS should be outside of the PLC particles as evident from negative surface charge, the immune modulatory activity was not hindered. Although PTX is known to activate macrophages to secrete TNF- α , the concentration of the drug needed (3 μM) (42) for the secretion of a measurable quantity of the cytokine is much higher than that delivered in this experiment (0.4 μM ; highest amount of

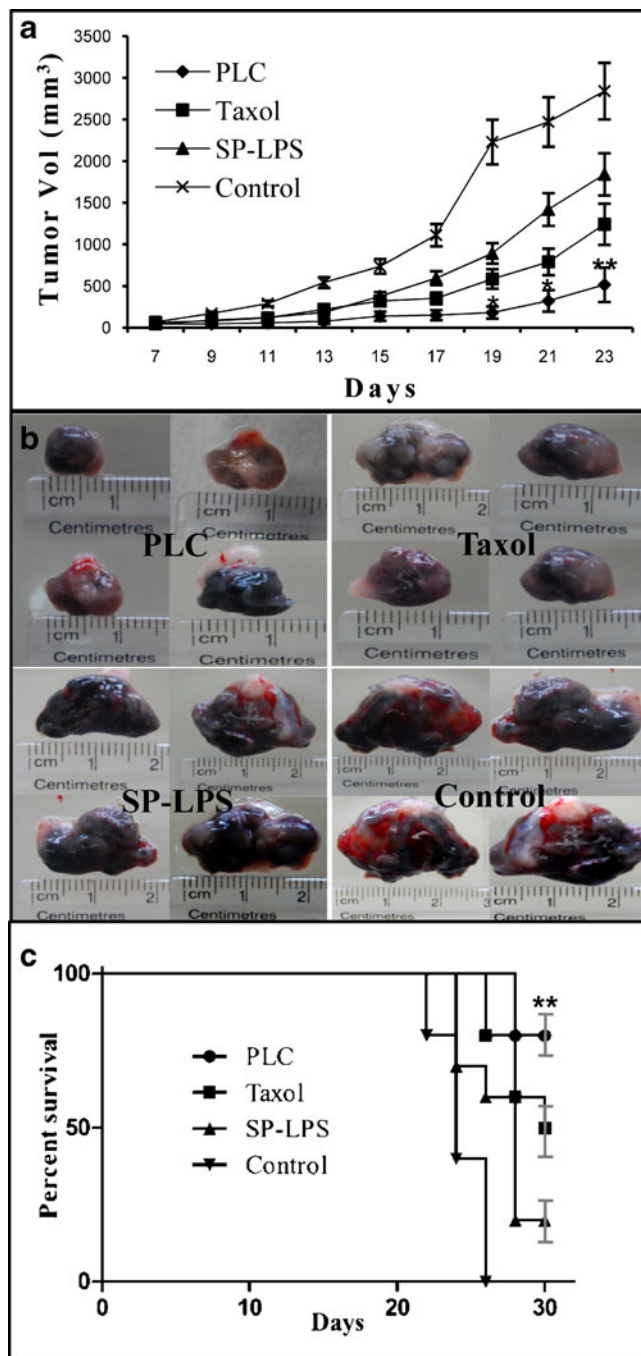


Fig. 8 Comparison of *in vivo* anti-tumor activity of PLC with Taxol and SP-LPS. Tumors were implanted by s.c. injection of B16-F10 cells in C57BL/6 mice. Each animal was administered with either Taxol® containing 100 µg PTX, or PLC containing equivalent amount of PTX or 100 µg SP-LPS or saline (control). 8 animals were taken in each group. Total 5 injections were given starting from day 7 after tumor implantation with an interval of 3 days. **(a)** Mean tumor volume \pm SEM at indicated time points in different groups of treated mice. **(b)** Representative images of excised tumors from different groups on 24th day after tumor implantation. **(c)** Comparison of survival of different groups of treated mice for 30 days. 10 animals per group were treated as mentioned above and observed for 30 days for mortality. Survival statistics was analyzed using Kaplan-Meier method. Anti-tumor activity of PLC was found to be significantly higher compared to both Taxol® and SP-LPS, which was also reflected in the better survival of the PLC treated mice. * $p < 0.1$; ** $p < 0.05$ values compared with Taxol treatment.

PTX present in PLC delivering 0.5 µg/mL SP-LPS). Hence, expectedly, there was no significant difference in the amount of TNF- α released between the SP-LPS and PLC treated groups. To confirm whether the macrophages activated by PLC were in turn able to stimulate the effector arm of the immune system, activation of splenocytes was evaluated. Splenocytes have all types of immune cells and the cross talk between macrophages and T cells and macrophage mediated T cell activation can be analyzed by examining their activation. Activated macrophages secrete IL-12, which further activates T cells. Significantly high amount of both IL-12 and IFN- γ was detected with PLC as well as SP-LPS treatment compared to control and PTX treated groups. These results provide evidence that macrophages activated by the action of PLC further stimulated the T cells for effector activity.

The co-culture study, which was *in vitro* model system of *in vivo* situation, confirmed the hypothesis of combined chemo-immunotherapeutic activity of PLC. Compared to the direct cytotoxicity experiment, where PLC and PTX treatment was given on cancer cells alone and similar death was observed with both the treatment, in the co-culture experiment where a mixed culture of cancer cells and splenocytes (which mimics *in vivo* situation) were treated, higher death of the cancer cells was observed with PLC treatment, as compared to PTX alone. In this experiment, the higher death of the cancer cells could be attributed to the immune stimulatory activity of PLC as PLC has been shown to induce TNF- α secretion from splenocytes which has direct cytotoxic activity. Activated cytotoxic T cells, present in the splenocytes, could also have contributed to the death of the cancer cells.

In vivo anticancer activity of the conjugate was found to be higher as compared to the individual components alone, confirming the hypothesis of better management of cancer with combined chemo-immunotherapy. Yao Ma *et al.* reported the synthesis and antitumor activity of a PTX – TLR4 agonist conjugate (PTX – muramyl dipeptide analogue conjugate) (43). Although their conjugate exhibited similar cytotoxic activity in *in vitro* studies and prevented metastasis, there was no significant difference between the tumor growth of PTX and conjugate treated animal (43). Furthermore, although they showed reduction in the number of immune suppressor cells in the spleen and bone marrow of the conjugate treated mice, no data regarding the immune status at the tumor microenvironment was produced. In our study, PLC treated animals exhibited significantly less tumor growth compared to PTX treatment ($p < 0.05$). The higher antitumor activity of PLC also resulted in better survival of the treated mice.

To understand the mechanism for better anticancer activity of PLC, the immune status of the tumor microenvironment was studied. Infiltration and activation of macrophages (CD14+ cells) and T cells (CD4+ and CD8+

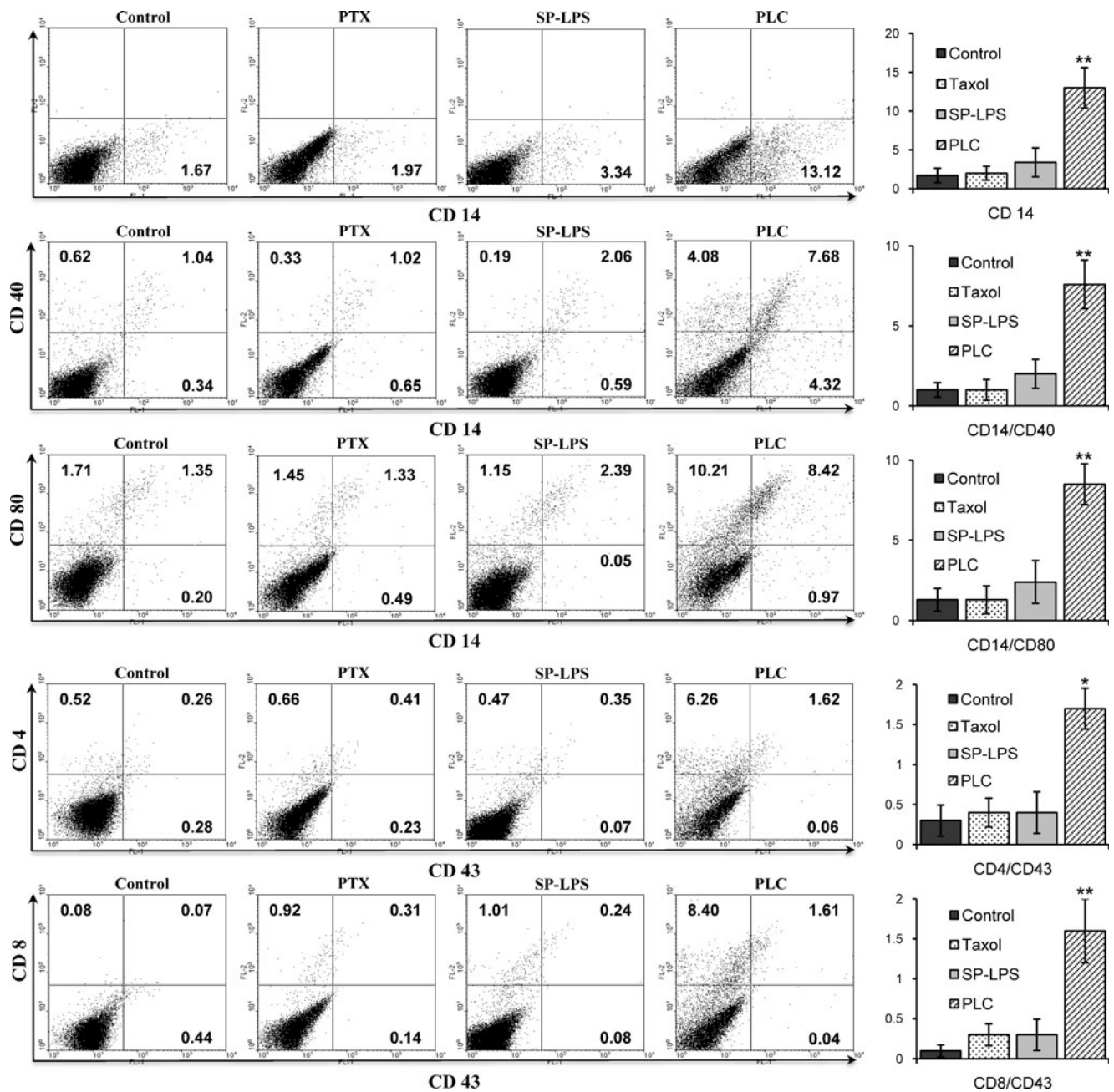


Fig. 9 Phenotypic characterization of tumor infiltrating mononuclear cells. Tumors were excised on 24th day after implantation from mice treated with PLC or Taxol® or SP-LPS. Mononuclear cells were isolated from the excised tumor and analyzed by flow cytometry. Bar chart indicate mean percentage of respective cells calculated from 3 set of experiments with \pm SEM. Significantly higher infiltration of activated macrophages and T cells was observed in the tumor of PLC treated animals compared to both Taxol® or SP-LPS treatment. * $p < 0.05$; ** $p < 0.01$, values compared with Taxol® treated group.

cells) were evaluated by isolation of tumor infiltrating immune cells and FACS analysis. In general higher infiltration of activated immune cells correlates with regression of tumor. We found significantly higher infiltration and activation of macrophages in the tumors of PLC treated animals compared to all other treatment groups. Macrophage activation at the tumor site is associated with tumor regression as reported by earlier studies (44). Percentage of CD40⁺ macrophages (CD14⁺/CD40⁺), which is a marker of M1

type macrophage, was also significantly higher in the PLC treated animals. Furthermore, significantly higher infiltration of activated CD4⁺ and CD8⁺ T cells were also seen with PLC treatment, which is known to be associated with tumor suppression (45). These data indicates that PLC treatment can effectively induce both stimulator and effector immune cells at the tumor microenvironment. Surprisingly, in the SP-LPS treated group, infiltration of immune cells and their activation was not significantly different as

compared to control group. Results of this study provide evidence of synergistic activity of chemotherapeutic drug and immunostimulator in the conjugate as treatment with Taxol or SP-LPS alone did not induce any significant increase in the number or activation of immune cells compared to the control group, whereas with PLC treatment, there was significant increase in the proportion of activated immune cells in the tumor microenvironment. As PTX present in PLC killed cancer cells via the apoptotic pathway and apoptotic bodies, which are good source of tumor antigens, are produced in that process, treatment with PLC would make tumor antigens available to the antigen presenting cells which in turn stimulate tumor antigen specific lymphocytes. Presence of SP-LPS in the conjugate would further activate these immune cells and thus induce strong anti-tumor immune response and exhibit a synergistic effect. Taken together these results suggest the development of a novel chemo-immunotherapeutic compound which has the potential to open up new avenues for cancer therapy in the near future.

ACKNOWLEDGMENTS & DISCLOSURES

This work was supported by the NII core grant. We sincerely thank Dr. Monica Sund for helping in the NMR studies. We are also thankful to the Advanced Instrumentation Research Facility of Jawaharlal Nehru University, New Delhi for the IR studies.

REFERENCES

- Morgan G, Ward R, Barton M. The contribution of cytotoxic chemotherapy to 5-year survival in adult malignancies. *Clin Oncol (R Coll Radiol)*. 2004;16:549–60.
- Emens LA. Chemoimmunotherapy. *Cancer J*. 2010;16:295–303.
- Hsiao JR, Leu SF, Huang BM. Apoptotic mechanism of paclitaxel-induced cell death in human head and neck tumor cell lines. *J Oral Pathol Med*. 2009;38:188–97.
- Szebeni J, Muggia FM, Alving CR. Complement activation by Cremophor EL as a possible contributor to hypersensitivity to paclitaxel: an *in vitro* study. *J Natl Cancer Inst*. 1998;90:300–6.
- Kan P, Chen ZB, Lee CJ, Chu IM. Development of nonionic surfactant/phospholipid o/w emulsion as a paclitaxel delivery system. *J Control Release*. 1999;58:271–8.
- Sharma A, Straubinger RM. Novel taxol formulations: preparation and characterization of taxol-containing liposomes. *Pharm Res*. 1994;11:889–96.
- Liggins RT, Burt HM. Polyether-polyester diblock copolymers for the preparation of paclitaxel loaded polymeric micelle formulations. *Adv Drug Deliv Rev*. 2002;54:191–202.
- Feng SS, Mu L, Win KY, Huang G. Nanoparticles of biodegradable polymers for clinical administration of paclitaxel. *Curr Med Chem*. 2004;11:413–24.
- Deutsch HM, Glinski JA, Hernandez M, Haugwitz RD, Narayanan VL, Suffness M, Zalkow LH. Synthesis of congeners and prodrugs. 3. Water-soluble prodrugs of taxol with potent antitumor activity. *J Med Chem*. 1989;32:788–92.
- Greenwald RB, Gilbert CW, Pendri A, Conover CD, Xia J, Martinez A. Drug delivery systems: water soluble taxol 2'-poly (ethylene glycol) ester prodrugs-design and *in vivo* effectiveness. *J Med Chem*. 1996;39:424–31.
- Li C, Yu DF, Newman RA, Cabral F, Stephens LC, Hunter N, Milas L, Wallace S. Complete regression of well-established tumors using a novel water-soluble poly(L-glutamic acid)-paclitaxel conjugate. *Cancer Res*. 1998;58:2404–9.
- Dosio F, Brusa P, Crosasso P, Arpicco S, Cattel L. Preparation, characterization and properties *in vitro* and *in vivo* of a paclitaxel-albumin conjugate. *J Control Release*. 1997;47:293–304.
- Dunn GP, Bruce AT, Ikeda H, Old LJ, Schreiber RD. Cancer immunoediting: from immunosurveillance to tumor escape. *Nat Immunol*. 2002;3:991–8.
- Roy A, Singh MS, Upadhyay P, Bhaskar S. Combined chemo-immunotherapy as a prospective strategy to combat cancer: a nanoparticle based approach. *Mol Pharmaceutics*. 2010;7:1778–88.
- Ailawadhi S, Sunga A, Rajput A, Yang GY, Smith J, Fakih M. Chemotherapy-induced carcinoembryonic antigen surge in patients with metastatic colorectal cancer. *Oncology*. 2006;70:49–53.
- Menard C, Martin F, Apetoh L, Bouyer F, Ghiringhelli F. Cancer chemotherapy: not only a direct cytotoxic effect, but also an adjuvant for antitumor immunity. *Cancer Immunol Immunother*. 2008;57:1579–87.
- Jassar AS, Suzuki E, Kapoor V, Sun J, Silverberg MB, Cheung L, Burdick MD, Strieter RM, Ching LM, Kaiser LR, Albelda SM. Activation of tumor-associated macrophages by the vascular disrupting agent 5,6-dimethylxanthone-4-acetic acid induces an effective CD8+ T-cell-mediated antitumor immune response in murine models of lung cancer and mesothelioma. *Cancer Res*. 2005;65:11752–61.
- Shinohara H, Yano S, Bucana CD, Fidler IJ. Induction of chemokine secretion and enhancement of contact-dependent macrophage cytotoxicity by engineered expression of granulocyte-macrophage colony-stimulating factor in human colon cancer cells. *J Immunol*. 2000;164:2728–37.
- Condeelis J, Pollard JW. Macrophages: obligate partners for tumor cell migration, invasion, and metastasis. *Cell*. 2006;124:263–6.
- Gordon S. Alternative activation of macrophages. *Nat Rev Immunol*. 2003;3:23–35.
- Mantovani A, Sica A, Sozzani S, Allavena P, Vecchi A, Locati M. The chemokine system in diverse forms of macrophage activation and polarization. *Trends Immunol*. 2004;25:677–86.
- Balkwill F, Charles KA, Mantovani A. Smoldering and polarized inflammation in the initiation and promotion of malignant disease. *Cancer Cell*. 2005;7:211–7.
- Garay RP, Viens P, Bauer J, Normier G, Bardou M, Jeannin JF, Chiavaroli C. Cancer relapse under chemotherapy: why TLR2/4 receptor agonists can help. *Eur J Pharmacol*. 2007;563:1–17.
- McIntire FC, Hargie MP, Schenck JR, Finley RA, Sievert HW, Rietschel ET, Rosenstreich DL. Biologic properties of nontoxic derivatives of a lipopolysaccharide from *Escherichia coli* K235. *J Immunol*. 1976;117:674–8.
- McIntire FC, Sievert HW, Barlow GH, Finley RA, Lee AY. Chemical, physical, biological properties of a lipopolysaccharide from *Escherichia coli* K-235. *Biochemistry*. 1967;6:2363–72.
- Schenck JR, Hargie MP, Brown MS, Ebert DS, Yoo AL, McIntire FC. The enhancement of antibody formation by *Escherichia coli* lipopolysaccharide and detoxified derivatives. *J Immunol*. 1969;102:1411–22.
- Shah S, Raghupathy R, Singh O, Talwar GP, Sodhi A. Prior immunity to a carrier enhances antibody responses to hCG in recipients of an hCG-carrier conjugate vaccine. *Vaccine*. 1999;17:3116–23.

28. Neises B, Steglich W. Simple method for the esterification of carboxylic acids. *Angew Chem Int Ed Engl*. 1978;17:522–4.
29. Chen JZ, Ranade SV, Xie XQ. NMR characterization of paclitaxel/poly (styrene-isobutylene-styrene) formulations. *Int J Pharm*. 2005;305:129–44.
30. Renuga Devi TS, Gayathri S. FTIR And FT-Raman spectral analysis of Paclitaxel drugs. *International Journal of Pharmaceutical Sciences Review and Research*. 2010;2:106–10.
31. Kooter IM, Pierik AJ, Merckx M, Averill BA, Moguilevsky N, Bollen A, Wever R. Difference fourier transform infrared evidence for ester bonds linking the heme group in myeloperoxidase, lactoperoxidase, and eosinophil peroxidase. *J Am Chem Soc*. 1997; 119:11542–3.
32. Dordunoo SK, Burt HM. Solubility and stability of taxol: effects of buffers and cyclodextrins. *Int J Pharm*. 1996;133:191–201.
33. MacEachern-Keith GJ, Wagner Butterfield IJ, Incorvia Mattina MJ. Paclitaxel stability in solution. *Anal Chem*. 1997;69:72–7.
34. Li X, Yu J, Xu S, Wang N, Yang H, Yan Z, Cheng G, Liu G. Chemical conjugation of muramyl dipeptide and paclitaxel to explore the combination of immunotherapy and chemotherapy for cancer. *Glycoconj J*. 2008;25:415–25.
35. Eralp Y, Wang X, Wang JP, Maughan MF, Polo JM, Lachman LB. Doxorubicin and paclitaxel enhance the antitumor efficacy of vaccines directed against HER 2/neu in a murine mammary carcinoma model. *Breast Cancer Res*. 2004;6: R275–83.
36. Zhong H, Han B, Tourkova IL, Lokshin A, Rosenbloom A, Shurin MR, Shurin GV. Low-dose paclitaxel prior to intratumoral dendritic cell vaccine modulates intratumoral cytokine network and lung cancer growth. *Clin Cancer Res*. 2007;13:5455–62.
37. Kingston DG. Taxol: the chemistry and structure-activity relationships of a novel anticancer agent. *Trends Biotechnol*. 1994; 12:222–7.
38. Rosler A, Vandermeulen GW, Klok HA. Advanced drug delivery devices via self-assembly of amphiphilic block copolymers. *Adv Drug Deliv Rev*. 2001;53:95–108.
39. Xin D, Wang Y, Xiang J. The use of amino acid linkers in the conjugation of paclitaxel with hyaluronic acid as drug delivery system: synthesis, self-assembled property, drug release, and *in vitro* efficiency. *Pharm Res*. 2010;27:380–9.
40. Wang Y, Xin D, Liu K, Zhu M, Xiang J. Heparin-paclitaxel conjugates as drug delivery system: synthesis, self-assembly property, drug release, and antitumor activity. *Bioconj Chem*. 2009; 20:2214–21.
41. Lemarchand C, Gref R, Passirani C, Garcion E, Petri B, Muller R, Costantini D, Couvreur P. Influence of polysaccharide coating on the interactions of nanoparticles with biological systems. *Biomaterials*. 2006;27:108–18.
42. Manthey CL, Brandes ME, Perera PY, Vogel SN. Taxol increases steady-state levels of lipopolysaccharide-inducible genes and protein-tyrosine phosphorylation in murine macrophages. *J Immunol*. 1992;149:2459–65.
43. Ma Y, Zhao N, Liu G. Conjugate (MTC-220) of muramyl dipeptide analogue and paclitaxel prevents both tumor growth and metastasis in mice. *J Med Chem*. 2011;54:2767–77.
44. Hagemann T, Lawrence T, McNeish I, Charles KA, Kulbe H, Thompson RG, Robinson SC, Balkwill FR. “Re-educating” tumor-associated macrophages by targeting NF-kappaB. *J Exp Med*. 2008;205:1261–8.
45. Pardoll D. T cells take aim at cancer. *Proc Natl Acad Sci U S A*. 2002;99:15840–2.